Design and package of a $^{14}CO_2$ field analyzer The Global Monitor Platform (GMP)

Bruno D. V. Marino*[a], Michelle Bright[b], Glen Gronniger[b]
[a]Planetary Emissions Management, 458 Massachusetts Ave. Ste. 300, Cambridge, MA, USA 02139;
[b]National Secure Manufacturing Center (NSMC) operated** by Honeywell FM&T, LLC

ABSTRACT

Carbon Capture and Sequestration (CCS) is widely accepted as a means to reduce and eliminate the fossil fuel CO_2 (ff-CO_2) emissions from coal fired power plants. Success of CCS depends on near zero leakage rates over decadal time scales. Currently no commercial methods to determine leakage of ff-CO_2 are available. The Global Monitor Platform (GMP) field analyzer provides high precision analysis of CO_2 isotopes [^{12}C (99%), ^{13}C (<1%), ^{14}C ($1.2x10^{-10}$ %)] that can differentiate between fossil and biogenic CO_2 emissions. Fossil fuels contain no ^{14}C; their combustion should lower atmospheric amounts on local to global scales. There is a clear mandate for monitoring, verification and accounting (MVA) of CCS systems nationally and globally to verify CCS integrity, treaty verification (Kyoto Protocol) and to characterize the nuclear fuel cycle. Planetary Emissions Management (PEM), working with the National Secure Manufacturing Center (NSMC), has the goal of designing, ruggedizing and packaging the GMP for field deployment. The system will conduct atmosphere monitoring then adapt the system to monitor water and soil evaluations. Measuring $^{14}CO_2$ in real time will provide quantitative concentration data for ff-CO_2 in the atmosphere and CCS leakage detection. Initial results will be discussed along with design changes for improved detection sensitivity and manufacturability.

Keywords: Laser, Assembly, Analysis, Gas, Carbon, Design, Package

1. INTRODUCTION

The overall objective of this project is to develop a real-time commercially available system capable of detection and high precision analysis of CO_2 isotopes in air (without pre-concentration), soil and water. Considering the availability of the amount of each isotope normally in the atmosphere [^{12}C (99%), ^{13}C (<1%), ^{14}C (1.2x10-10%)] great emphasis on developing detection of the ^{14}C has been the area of focus with interest to improve the precision of ^{13}C detection. The system is comprised of three wavelength single mode tuned sealed-off gas lasers of each isotope of CO_2 with RF power supplies, sample and reference cells, oscillation and differential amplifier boards, low pressure/flow gas handling system, analyzing software, and packaging hardware. The sealed-off $^{14}CO_2$ laser design and operation is based on the seminal work of Freed and co-workers of the Lincoln Laboratory. These items and their functionality within the system will be discussed further along with system integration. The first portion of this report includes the science of the system concerning the optogalvanic (OG) detection system, lasers and cells function, signal output, and data comparisons in a lab environment. Secondly, the packaging of the system for initial field deployment will be reviewed with consideration of mechanical challenges, electrical concerns, environmental issues, and future improvements. Lastly, an overview of an integrated MVA process, the PEM system of systems, will be discussed in relation to overall system structure and how the data will be utilized for regulatory compliance and creation of carbon credits. The PEM system of systems refers to a spatial array of devices across targeted locations to monitor and verify leakage of geological sequestered CO_2 (GSC) at site related scales. The end product, the Global Monitoring Platform (GMP), is to provide a high resolution, low cost, spatial and temporal data for a direct marker of fossil fuel as a means to detect leakage of geologic sequestered CO_2, create verified tradable carbon credits, and expand to other needs as identified. The basic instrument design and initial platform used in this work resulted from a Phase I SBIR grant awarded to PEM Inc. in 2008.

*bruno.marino@pem-carbon.com; phone 1 617 842 5569; fax 1 207 781 3206; pem-carbon.com

**For the United States Department of Energy under contract No. DE-NA0000622

2. THE SCIENCE

2.1 Opto-Galvanic Detection System

Optogalvanic (OG) spectroscopy and applications to isotopic analysis have been previously reported[1] and more recently for $^{14}CO_2$[2]. The OG effect can be quantified by measuring current or voltage changes in electrical discharges (e.g., plasma) following laser irradiation at wavelengths corresponding to specific lasing transitions of the species in the discharge and is proportional to the absorbed laser power. The change observed in the conductivity of a gaseous discharge due to a resonant excitation is termed "the Opto-Galvanic Effect" (OGE)[3,4]. The OGE in this work is due to the perturbation of a plasma discharge by resonant laser excitation[5]. A good approximation of the OGE signal (S = conductivity change) and the variables corresponding is shown in equation (1)[6].

$$S = nLIA\sigma C \text{ where,} \tag{1}$$

n = average molecular density
L = interaction region length
I = average laser intensity
A = average cross-sectional area of laser beam
σ = Laser species interaction cross section
C = proportionality constant for OGE

Moreover, the OG effect is also proportional to the density of the absorbing species.[7] Here we are concerned with isotopic-ratio spectroscopy in which the determination of the ratios $R_{\alpha\beta}=\alpha N/\beta N$ of any two isotopic pairs α and β of an element by OG spectroscopy typically consists of measuring the densities of the two isotopes. To relate $\alpha N/\beta N$ to the laser-induced OG signal we consider a specific lasing transition with wavelength λ_0 in which the OG signal at the frequency v for the selected transition, S(v), is related to the absorbed laser intensity ΔI(v) according to:

$$S(v) = CD\Delta I(v) \text{ where,} \tag{2}$$

D = geometrical cross section of the laser beam
C = proportionality factor that is constant for a given specified transition

Where the absorber is of length l is illuminated by the laser beam of intensity I_0 (2) becomes:

$$S(v) = CDIo\{1 - \exp[-k(v)l]\} \text{ where,} \tag{3}$$

k(v) is the frequency dependent absorption profile of the selected transition.

Equation (3) can be further reduced to:

$$S(v) = CI_0Dk(v)l \tag{4}$$

Thus, an optimized OG detection system is sensitive to laser intensity (I_0) and interaction length (l)[8] as well to the proportionality constant (assumed to be the same for a given lasing transition)[9]. Contained within this equation is the clear need for a high level of control of temperature, pressure and flow-rate to the OG detector. These parameters can affect the output signal and must be monitored and controlled so that changes in the OG detection system due to technical noise does not become confused with changes based on the differences in the isotopic concentrations and their subsequent signals. We have observed directly that system misalignment can cause temperature dependent effects directly correlated to the chopping frequency of the lasers. This has the implications that data obtained my not just be

due to the OGE but also to temperature dependent effects. Temperature effects are particularly important for field work environments that may range from Arctic to desert environmental conditions.

2.2 Lasers and cells

The current setup is shown schematically in Figure 1. The major components in the layout are as follows: three (3) CO_2 lasers of three different carbon species, two reference cells, and two sample cells. The three laser species; $^{12}CO_2$, $^{13}CO_2$, and $^{14}CO_2$, are used to probe and provide excitation to the appropriate sample and reference cells. Each laser species corresponds to the resonant excitation of the reference and sample cells for the designated or unknown carbon isotope within the cells. For example, the ^{12}C and ^{13}C reference cell contains known amounts of these isotopes, when probed with the resonant laser excitation direct correlations can be drawn to quantify the amount of electric conductivity change with respect to the quantity of isotope present. The reference cells allow for a check of these amounts, while the sample cells contain or flow the unknown isotopic concentrations. The resonant effect in the plasma discharge is highly dependent on the laser species used. Strict line stabilization in the lasers[10] must be maintained for proper excitation stability with respect to the isotope of interest. All three lasers rely on a piezoelectric transducer (PZT) for stabilization and the feedback mechanism utilized is the OGE itself[11] in the current system and is also an approach commonly used for CO_2 laser stabilization. The system relies on very common isotopic ratios[12 13 14] for data comparison and evaluation. For instance, the reference cell must contain known amounts of each isotopic concentration as this allows for a relative ratio to be determined and compared with that of the sample ratio, see equation 5. The delta value given in equation 5 represents a relative measurement of the isotopic ratio and allows for proper result comparisons between data runs.

$$\delta = \frac{R_{sample} - R_{s\tan dard}}{R_{s\tan dard}}(1000\delta\%) \tag{5}$$

The lasers are mechanically chopped to provide an identification of and separation of the two or three laser species present during operation. The frequency of the chopping causes the OG electrical signal to be modulated at the same frequency since the laser induced excitation is responsible for the OG signal. LabVIEW control allows for the Fourier transform of the OG signal to be evaluated and identified by laser species. The Fourier evaluation of the system allows the reference and/or sample cells to be excited by more than one laser species at a time; this assures that the same sample and/or reference mixture is probed by both lasers simultaneously.

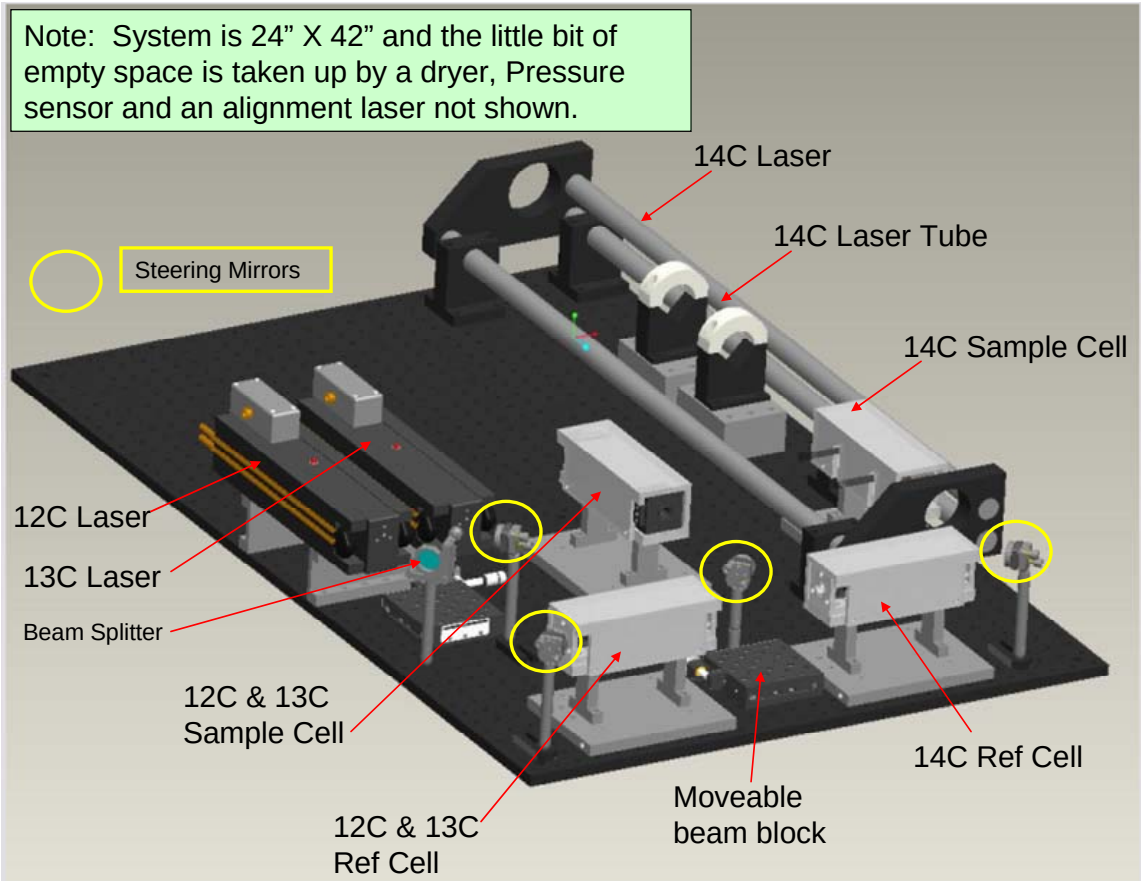

Figure 1. Schematic of System Layout

2.3 Signal output

The OG electric signal output from the system is used to calculate the delta values and determine relative isotopic concentrations. The real-time data output of the LabVIEW program gives an average of the OG output signal as shown in Figures 2 and 3. This OG signal changes amplitude based on the chopping frequency. As the laser is modulated from a position of on to off; the resonances in the plasma discharge changes amplitude. This result is evidence of the resonance dependence of the OG signal. The chopping frequencies are different for each laser species allowing for a separation of data and determination of relative amplitude and its variability over time for each isotope being investigated. Figures 2 and 3 show the real-time average data output for the ^{12}C and ^{13}C sample testing. The two plots in each figure allow for the comparison of the ratio of sample concentration (unknown OG signal amplitude) to the reference (known OG signal amplitude) concentration. Large amplitude does not necessarily lead to a high isotopic concentration as it must be compared to the reference to obtain the ratio and thus the proper relative concentration.

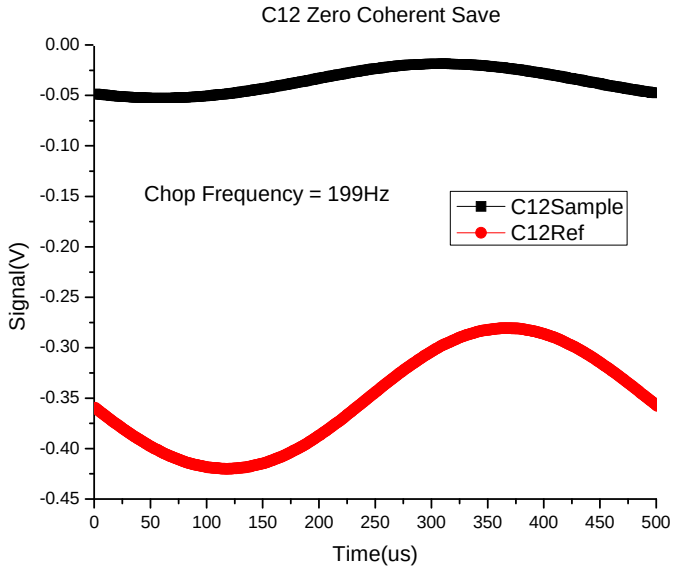

Figure 2. ^{12}C signal data for a nominal gas configuration.

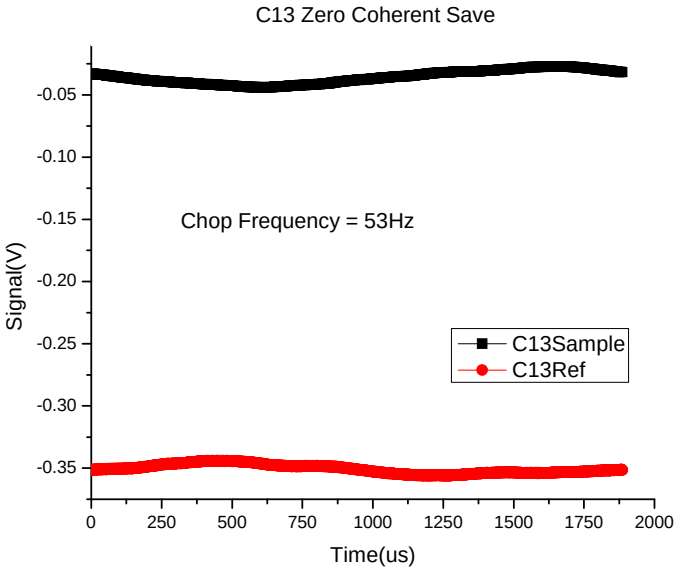

Figure 3. ^{13}C signal data for a nominal gas configuration.

2.4 Establishing data

Figure 4 shows a screen shot of representative system data. The time scale represents the scan length. The signals span different time spectra due to the fact that they are directly coupled to the laser chopping frequency. This real-time signal is then Fourier transformed so that the constant monitoring of the amplitude and its corresponding frequency can be

monitored. The screen shot shown represents many scans added together in the real-time window. If a resonance, and thus an isotope, is present there will be some level of amplitude modulation in the output signal observed on the screen. Once the sample output level is compared with the reference level and thus the known concentrations, the proper ratio can be established and provides a scaling for the individual runs. This scaling allows one to quantify a certain value of excitation (voltage in this case) to a specific isotopic concentration. This is essentially a built in calibration for individual runs. The frequencies can be chosen independently but specific frequencies must be separated by considerable intervals to prevent data overlap.

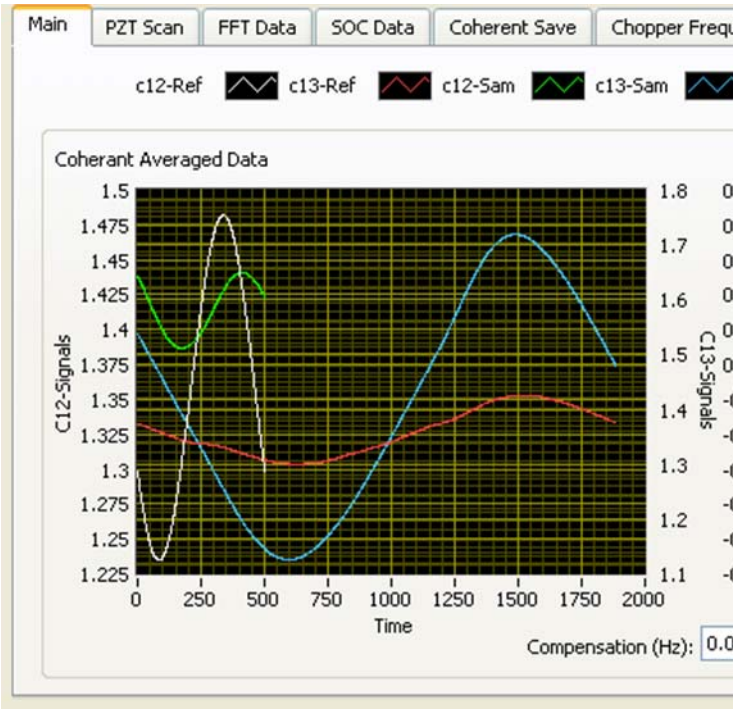

Figure 4. Screen Shot Data

3. PACKAGING

The initial system was produced as a result of a Small Business Innovation Research (SBIR) Phase 1 grant to PEM Incorporated. It was a lab unit positioned on an optical board with commercial off the shelf (COTS) lasers, optics, optical mounts and peripheral equipment. The challenges extended beyond opto-mechanical elements to chemical concerns, transmission, thermal, vibration, size, weight, hermetic and of course electrical characteristics considering RF noise and interference. Two of the lasers, ^{12}C & ^{13}C are commercially available packaged lasers; however, the ^{14}C laser was not and is therefore an open laser at the beginning of development. The ^{14}C laser was developed in conjunction with knowledge from Charles Freed and his legacy[10] with further improvements scheduled for the 2011 deployment. There is much work to be completed to optimize the ^{14}C sample cell to receive enough laser power to gather data that is capable of being analyzed with a considerable amount of precision and accuracy within a transportable and stable assembly. The entire system must be able to withstand a multitude of environments and transporting situations. The approach is to phase the packaging improvements into each prototype as they are developed and deployed. The overall objective is to eventually evolve the lab unit to a field deployable and rugged system with interchangeable modules for ease of maintenance and in situ requirements.

3.1 Mechanical

The lasers and optics must be stabilized and kept from debris, condensation and extreme heat. In order to accomplish the need to have the main components within a limited footprint while maintaining functionality of the optical assembly in a field environment the first step was to reconfigure the system. This led to the design of individual custom mounts for the cells, lasers and mirrors to keep the laser beams and their alignment in one plane. Before coming to the configuration as seen in Figure 1, the team evaluated other layouts as seen in Figures 5-7 as well as the layout in Figure 1. The first step was to take the original layout and rotate one of the lasers so that the ^{12}C and ^{13}C lasers pointed in the same direction and both would hit the same cell at the same time as shown in Figure 5. This configuration allowed for easier alignment and monitoring of laser power, provided system symmetry, and was more convenient for the addition of the ^{14}C laser. The disadvantage was in being able to directly compare data with the original system. To compensate for this disadvantage, data runs were completed in a specifically created process to assure that the functionality and integrity of the system was not lost. Next the incorporation of the ^{14}C laser was laid out as seen in Figures 6 and 7. Figure 6 allowed for the use of a single reference cell and single sample cell which would allow for the smallest system footprint and ability to monitor all ratios at the same time. Considering that at the time of development a ^{14}C laser was not available, it was unclear if enough laser power would be transmitted through the output coupler for ^{13}C signal readings. This led to the configuration shown in Figure 7, which is a similar layout that has the added advantages of very easy alignment and no ^{13}C laser power issues; however it doesn't allow for detection of ^{13}C and ^{14}C at the same time. Other disadvantages are temperature differentials between separate sample cells, addition of moveable components and ensuring sample cells are equivalent in concentration. With all layouts having been taken into consideration the final layout of Figure 1 was agreed upon by the team for its ability to fit into the footprint required, allow for detection of ^{13}C and ^{14}C at the same time, and ease of alignment. Custom mounts were designed and made to hold the lasers, optics and cells at the same height and plane to provide for general laser safety and ease of alignment. The sample cell and reference cell were mounted separately and in a phenolic mount to reduce stress and thermal effects. The whole system as seen in Figure 1 was then placed into a rugged commercially available case that was adapted to hold the optical breadboard and placed on a cart with shock absorbers for transportation as shown in Figure 8 item 1.

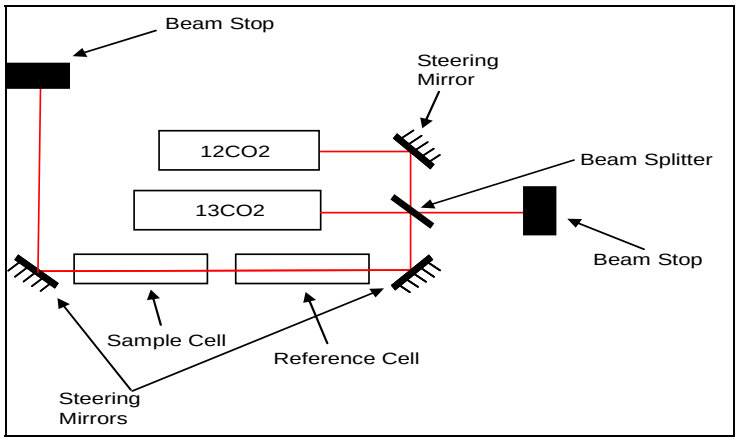

Figure 5. Layout representative of initial lab unit

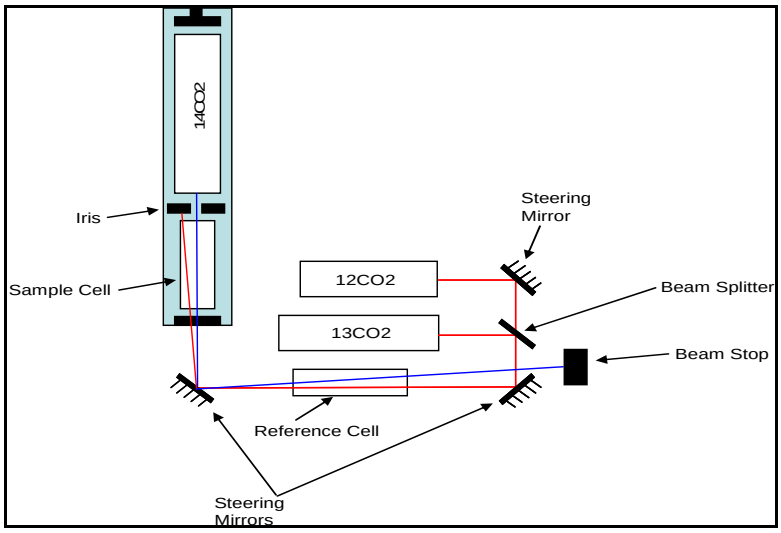

Figure 6. Final Layout Option #1

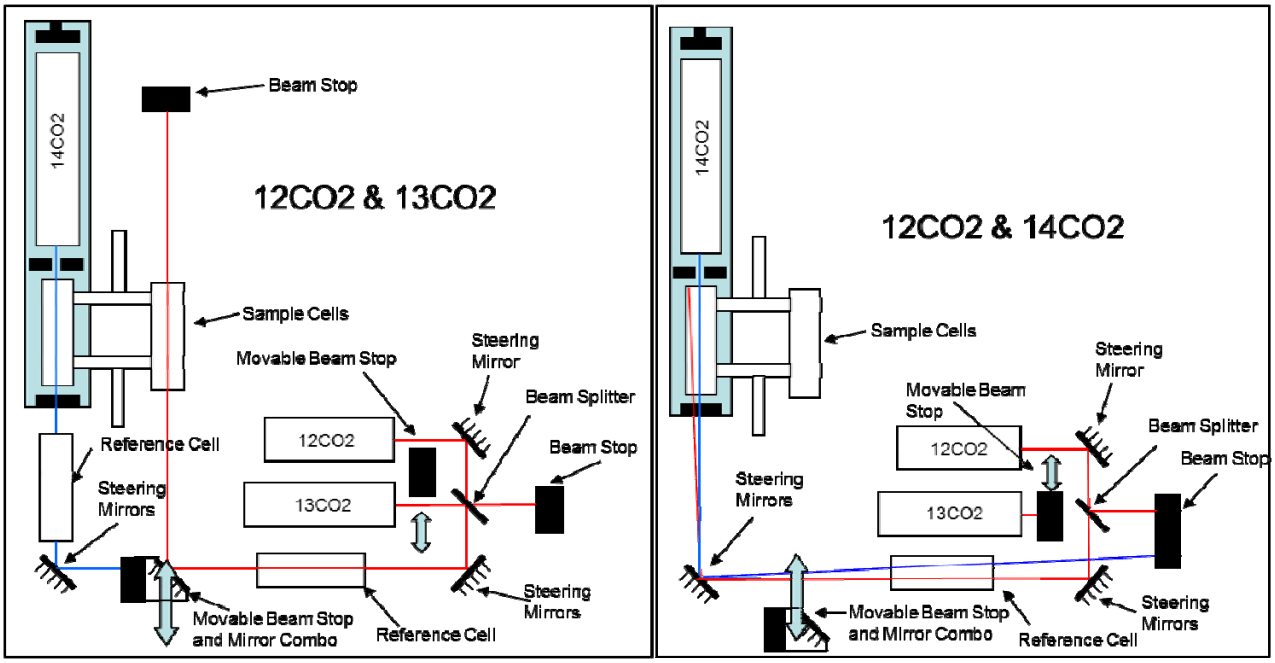

Figure 7. Final Layout Option #2

Figure 8. Final layout package for deployment

3.2 Electrical and power

The need to ruggedize the system with electrical components wrapped in and around the lasers and other optics presented a number of thermal issues. The oscillation board and differential amplifier boards are kept as an assembly that are mounted with each cell and therefore need close proximity for function. The oscillation board provides a high frequency discharge that excites the gas in the cell producing plasma. The plasma color and visibility is dependent on the contents of the cell and the power transmitted via wire from the oscillation board to the copper tape surrounding the cell. The differential amplifier board retrieves the signal, amplifies it, and sends the signal to the LabVIEW program that creates a visual graph of the signal on a monitoring panel as seen in Figure 4. It was determined that separation of the power supplies (e.g. laser power supplies and field power) into separate assemblies, Figure 8 items 2-4 respectively, was required to manage the electrical thermal load. These items are connected to each other and the laser system by custom cables and a bulkhead plate that accommodates the various types of connections and insulation. The initial power supplies were not usable and until this could be redesigned and built, the team utilized power drawn from four large linear lab power supplies with a total weight of 103 lbs. and an envelope of 2 ft^3. Research of correct power supplies to support the needs of the system, cable shielding, noise filtering, control interfaces, efficiency and thermal properties had to all be considered. The power supply unit and laser power supply unit both had to be rugged, fully enclosed, light-weight, and most of all not introduce noise into the laser system. This was accomplished by designing a custom package with commercial power supplies and a modified zero case. The final power supply unit weight was 12 lbs. in an envelope of 1 ft^3 and was easier to use especially in a field environment as shown in Figure 9. The final laser power supply was similar in that a zero case was modified to fit the existing laser power supplies, with custom toggle switches and special cables as shown in Figure 10.

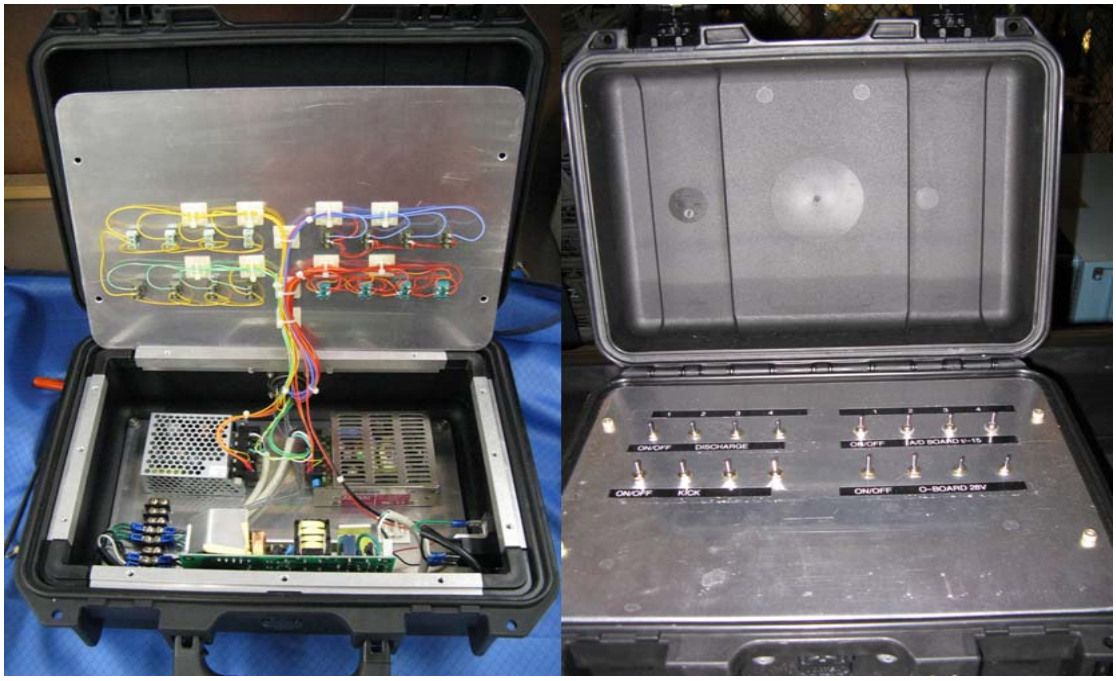

Figure 9. Power supply unit final package

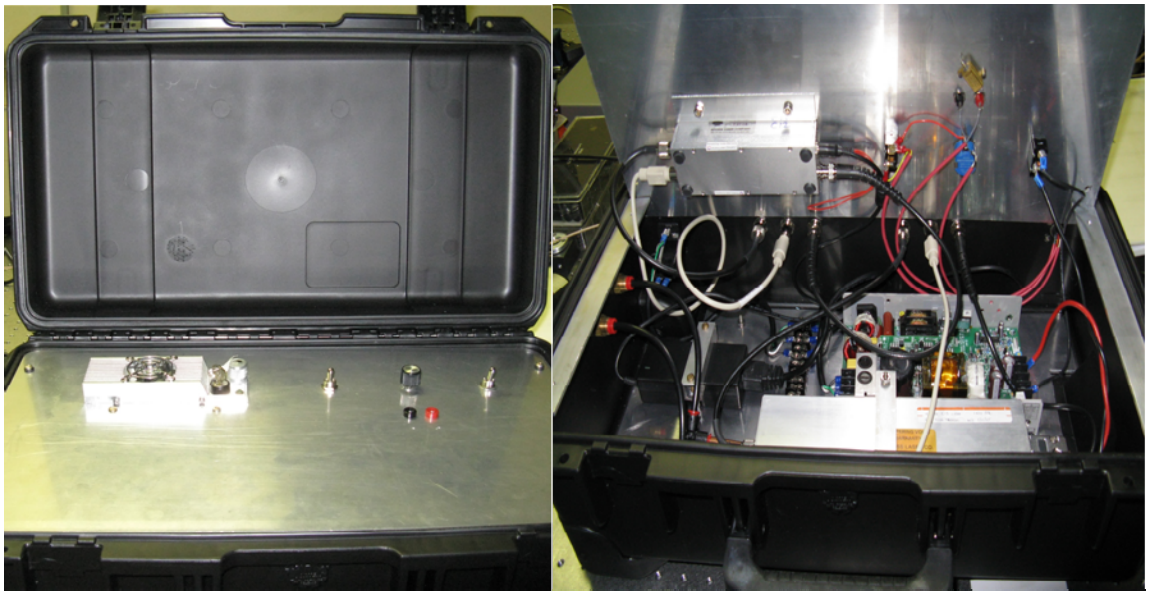

Figure 10. Laser power supply unit final package

3.3 Future upgrades

Initially there will be emphasis on improving the ^{14}C laser for stability and power output to include removal of the sample cell from inside the laser body (intra-cavity) to an external cell for ease of packaging and commercialization. Different configurations to ensure short and long term frequency stabilization will be investigated. The oscillation and differential amplifier boards require redesign to reduce noise and power consumption as well as upgrade to more readily available components. The pressure flow system consists of a mass flow controller, pressure transducer, and roughing pump as currently deployed. This will be redesigned to be integrated within the laser assembly and incorporate a dryer

for the incoming air to be sampled and to maintain a more consistent pressure and flow rate. Management of thermal load from the laser itself was controlled with a small lab chiller for present purposes. However, the addition of solid state chillers, fans, and redesign of heat sinks and heat flows will diminish and eventually eliminate the need for typical electric chillers.

4. SYSTEM OF SYSTEMS

4.1 Overview

The emergence of a market-based trading system for greenhouse gases (GHG), specifically as embodied in atmospheric CO_2, presents a technically more demanding and project specific approach relative to studies of the global carbon cycle. Cost-effective, high-precision and carbon-specific monitoring underpins not only our understanding of the carbon dynamics of the planet (e.g., full carbon budget) but is also the basis of the carbon economy with discrete geographically defined projects representing partial (local and regional) carbon budgets (e.g., Regional Greenhouse Gas Initiative[15], CA AB32 legislation[16]). An accounting of the carbon burden emitted at local, regional, country-wide and global scales is ideally mirrored in regulatory approaches to reduce, avoid and otherwise diminish current sources as well as show negative carbon emissions through carbon sequestration. However, markets have grown based on estimation not measurement of greenhouse gas emissions. In particular, no field-deployable commercial and geographic-scale system for the direct measurement, monitoring, verification and accounting (MVA) of carbon for the purposes of carbon trading is available introducing considerable uncertainty in the functioning of carbon markets, pricing and management strategies. PEM's system of systems[17] provides a commercial, geographic scale system for the integration of carbon flux from both natural and man-made carbon emissions, producing a dual carbon accounting system in which biogenic or natural and fossil/industrial emissions are quantified separately for the purposes of carbon trading. Thus, trading of carbon may be refined as a two-carbon approach (e.g., fossil fuel C and biogenic C), recognizing that both ecosystem function and anthropogenic actions may be differentially priced according to the efficiency of carbon reduction and other factors. The goal of the system of systems is to provide real time, quantitative analysis of isotopologues of atmospheric gases. The Global Monitor Platform, as described above, collects atmospheric gases, analyzes the gases for isotopic composition using a variety of isotopic analyzers over a range of sampling frequencies, and harmonizes data across sampling sites using standards and/or global references (e.g., National Oceanic and Atmospheric Administration). Data are provided to a central location and provide isotope-based data products according to model based conversion methods that result in metric tons of carbon appropriate for carbon trading exchanges. Such products in the case of CO_2 can result in a two carbon system (e.g., biogenic and fossil carbon) for trading that can be applied by industries, states, regions, governments, greenhouse gas exchanges, verification bodies for greenhouse gas treaties and by other stakeholders for use in carbon budget analysis, carbon pricing and carbon management. An overview of the system of systems is shown in Figure 11 including an ensemble of GMP analyzers across a landscape, telemetry of data (sample and standard values), database acquisition, processing and model analysis and final data products ready for carbon trading markets[18].

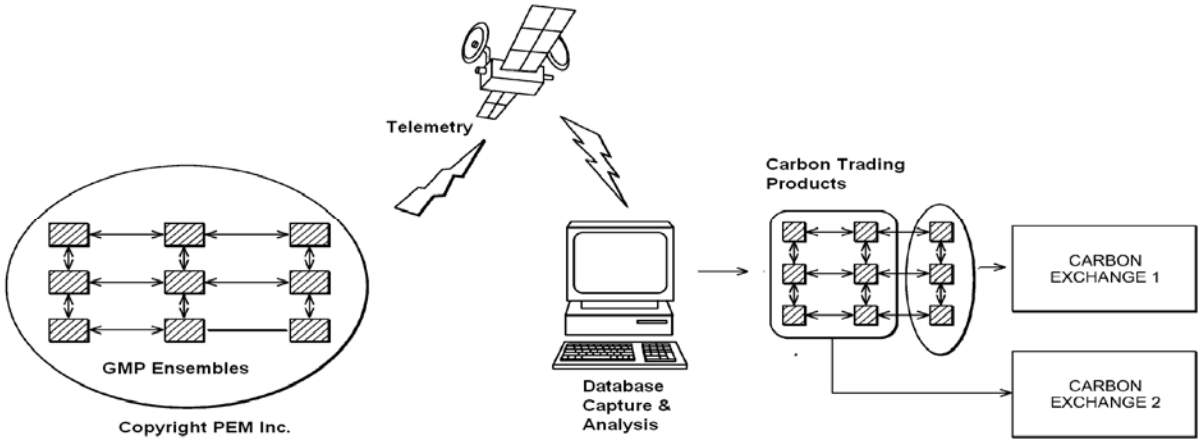

Figure 11. System of Systems Overview

4.2 Initial field results

The first continuous field measurements, obtained at one Hertz (1Hz) sample frequency, for $^{14}CO_2$ in the free atmosphere and in soil gas, have been completed using the GMP as described above. A total of approximately 5,000 ^{14}C values based on a NOAA reference gas standard curve (provisional) were made over three days illustrating the potential for a very high data rate for ^{14}C measurements in the field, a critical component of a carbon capture and sequestration (CCS) monitoring, verification and accounting paradigm. The GMP was deployed at Mammoth Mountain, Horseshoe Lake, CA, a well-known tree-kill site and high flux natural vents for magmatic CO_2 resulting from the Mammoth Mountain volcanic formation. A control site with established and healthy trees was also sampled with the GMP. The magmatic CO_2 source is known to be $^{14}CO_2$ free and representative of CO_2 derived from combustion of fossil fuels (ff-CO_2). In many cases this is a typical source of CCS injection gas and, if unaltered isotopically, of CO_2 leakage. Figure 12 shows the tree kill area (a), a view of Horse Shoe Lake (b) and a view of Mammoth Mountain (c). Figure 13 shows the field site environment with deployment of the GMP from a trailer (a), general work area where measurements were made showing also eddy covariance equipment (b) and a view of a soil gas chamber and solar panels (c). The GMP was operated with battery power for approximately six hours per sampling interval. $^{14}CO_2$ data for soil accumulation chambers was also obtained by sampling directly from the soil chamber air flow during normal operation of the soil chamber measurement routine demonstrating successful integration of soil chambers and the GMP analyzer. The soil chambers and associated control hardware and software were provided by LICOR Inc., Lincoln, NB. Soil data will be reported elsewhere. Eddy covariance data to determine the flux of CO_2 from the site have been reported but do not incorporate the isotopic data[19].

The field work resulted in successful demonstration of ^{14}C measurement technology transfer from the lab bench to the field and demonstrated good long term stability of laser output using sealed reference cells, constant pressure and gas flow rates of 10 sccm—critical for laser precision and accuracy. The field demonstration of a 3 point standard curve using NOAA characterized reference gases (0 fraction modern, 0.9 fraction modern, 1 fraction modern) provided for instantaneous conversion to $^{14}CO_2$ values. We emphasize the preliminary status of the standard curve analysis linking OG signals to the ^{14}C scale pending inclusion of additional analysis of NOAA reference gases. The field demonstration of continuous measurement of $^{14}CO_2$ in the free atmosphere of the Horse Shoe Lake and control site environments were in general agreement with expected values. Being able to map the OG raw data to gas standards of known isotopic composition by use of a direct and simple method will ensure successful standardization across all analyzers regardless of location. This is a critical requirement of the system of the systems GMP for landscape scale carbon accounting, carbon treaty verification, carbon fraud prevention and carbon trading networks. The use of modular sealed cells in the GMP units provides for easy replacement and or standardization with other primary, secondary or tertiary standard gases in sealed cells for use specifically in the GMP. The preparation of the sealed reference cells with known gas composition and pressure are under further development for commercialization and may be employed by other laser-based analyzers.

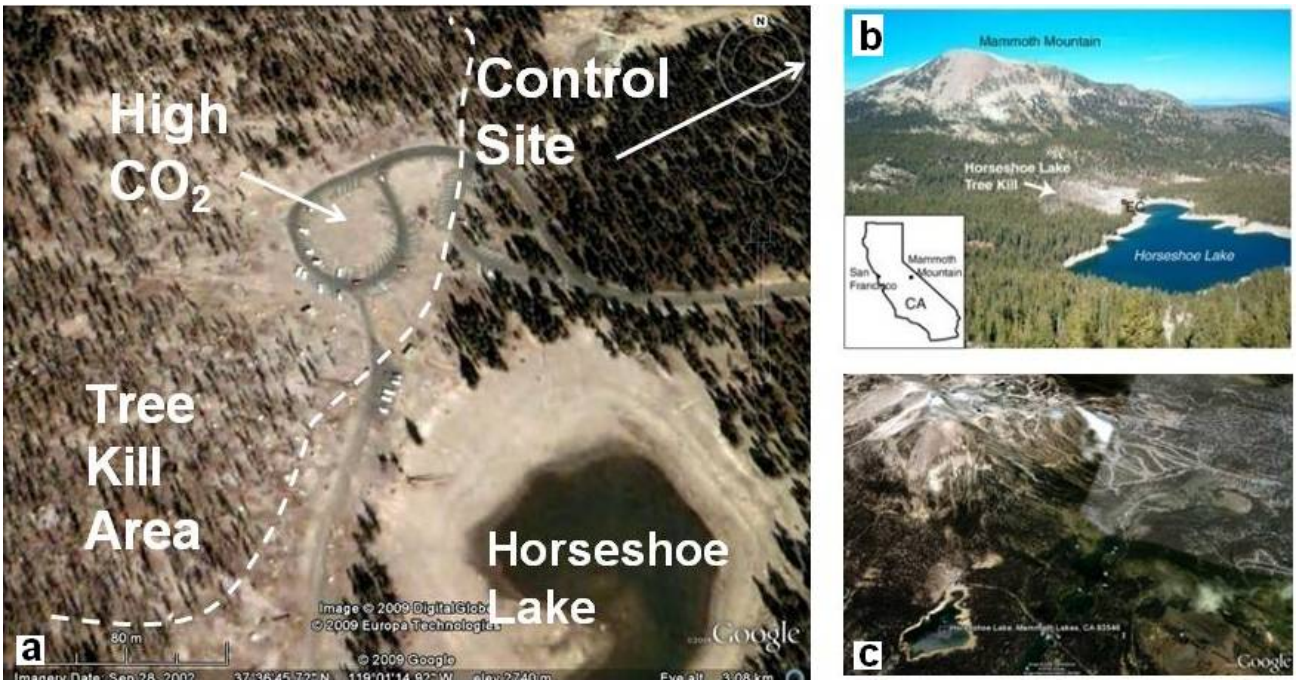

Figure 12. Field site location

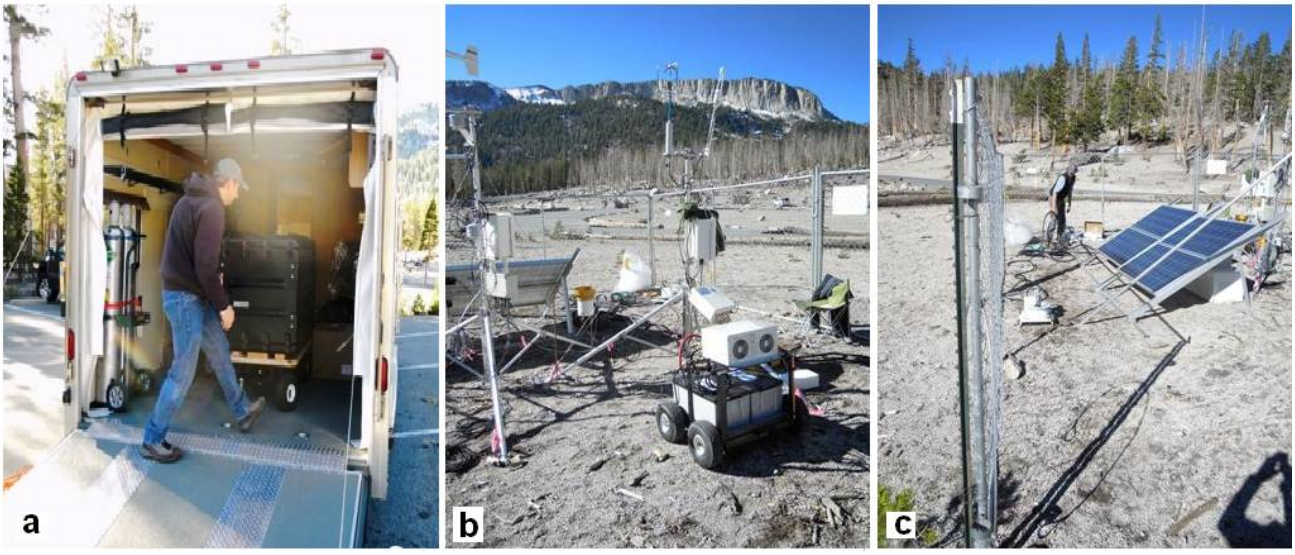

Figure 13. On site gathering data

Few data exist for $^{14}CO_2$ of Mammoth Mountain free atmosphere and soil gas. Mammoth Mountain ^{14}C atmospheric values were inferred from ^{14}C measurements on plant materials including tree rings from the Mammoth Mountain area[20]. Analyses of ^{14}C values for the atmosphere and their relationship to tree rings and plant material are well established from bomb radiocarbon data and current data for ^{14}C composition of plant material near nuclear power plants, a source of enriched $^{14}CO_2$[21]. Based on the available data, plant ^{14}C values are considered a reasonable direct estimate for the atmospheric values at the time of incorporation into the plant material and are used here for comparison with GMP measured values. Figure 14 shows a summary comparison of ^{14}C values for atmospheric data (A) from the Mammoth Mountain Horse Shoe Lake (HSL) site collected using the GMP and ^{14}C values derived from plant material (P) from the Mammoth Mountain background (BG) control site.[22] The GMP and plant values are in general agreement reflecting

depleted values for $^{14}CO_2$ within the HSL site, the area with high flux of ^{14}C free CO_2 from magmatic sources and for the background site representative of typical ambient $^{14}CO_2$ characteristic of the free atmosphere[23]. NOAA style flask samples were filled with ambient air in both the HSL and BG areas using a portable NOAA flask filling system for Accelerator Mass Spectrometry (AMS) analysis. The AMS data will be compared with the plant and GMP data in a future publication.

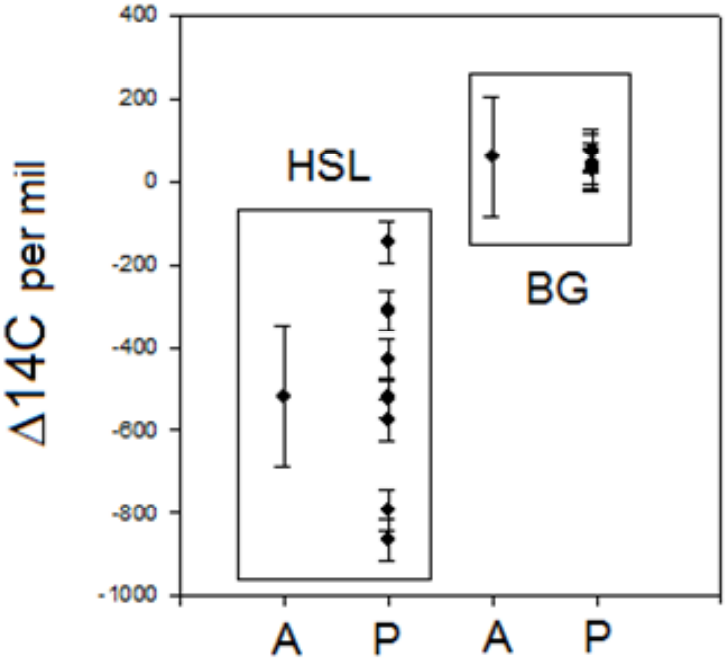

Figure 14. Summary of GMP and Plant Data for ^{14}C

5. SUMMARY

A field ready analyzer for atmospheric $^{14}CO_2$ has been successfully transferred from the lab bench setting. Initial results demonstrate the feasibility of the approach using gas filled lasers and sealed reference gases. The single deployment of the GMP will be followed up by deployment of multiple instruments in selected areas and ultimately within an operating CCS facility. The GMP will proceed through a series of maturation phases increasing the GMP technology readiness level at each phase. The initial deployment revealed a number of areas that require improvement including short term laser stability, increased frequency stabilization, and the use of additional NOAA characterized standard gases in the field. Assuming improvements in GMP performance as maturation proceeds, the deployment of ensembles of GMPs in the field in a CCS setting will offer key features for success of CCS including:

1) Improvement in the understanding of storage processes and confirmation of their permanence; 2) Enabling a sensitive indicator of potential damage to the host flora, fauna and ecosystem level processes; 3) Enabling the assessment of environmental, safety and health (ES&H) impacts in the event of a leak to the atmosphere or shallow source of surface or ground water; 4) Providing a baseline and tracking tools to evaluate and monitor any required remediation efforts should a leak occur; 6) Providing a basis for verified emissions reduction credits of CCS and their financial integration with carbon trading and compliance frameworks worldwide; 8) Providing comparable system-level information of single and multiple CCS projects offering feedback, improvement and risk reduction practices to project operators, policy makers and technologists.

REFERENCES

[1] Pianarosa, P., Demers, Y., and Gagné, J. M., "Isotopic analysis by optogalvanic spectroscopy," Journal of the Optical Society of America, B 1, No. 5, 704 (1984), http://www.opticsinfobase.org/abstract.cfm?URI=josab-1-5-704

[2] Murnick, D. E., Dogru, O. and Ilkmen, E., "Intracavity optogalvanic spectroscopy, a new ultra-sensitive analytical technique for ^{14}C analysis," Analytical Chemistry 80, No. 13, 4820-4 (2008), http://www.pubmedcentral.nih.gov/articlerender.fcgi?artid=2770733&tool=pmcentrez&rendertype=abstract

[3] Penning, F.M., "The action of positive ions in an independent gas discharge," Physica, 8, 137 (1928).

[4] Beniamino, B. and Beverini, N., "Optogalvanic spectroscopy," Reviews of Modern Physics, No. 3, 62 (1990).

[5] Lawler, J.E., "Experimental and theoretical investigation of the optogalvanic effect in the helium positive column," Phys. Rev. A, 22, 1025 (1980).

[6] Murnick, D. and Okil, J., "Use of the optogalvanic effect (OGE) for isotope ratio spectrometry of 13CO2 and 14CO2," Isotopes in Environmental and Health Studies, No.4, 41 (2005).

[7] Pianarosa, P., Demers, Y., and Gagné J. M., "Isotopic analysis by optogalvanic spectroscopy," Journal of the Optical Society of America, B 1, No. 5, 704 (1984), http://www.opticsinfobase.org/abstract.cfm?URI=josab-1-5-704

[8] Pianarosa, P., Demers, Y., and Gagné J. M., "Isotopic analysis by optogalvanic spectroscopy," Journal of the Optical Society of America, B 1, No. 5, 704 (1984), http://www.opticsinfobase.org/abstract.cfm?URI=josab-1-5-704

[9] Barbieri, B., Beverini, N. and Sasso, A., "Optogalvanic spectroscopy," Reviews of Modern Physics, Vol. 62(3), 603, (1990).

[10] Freed, C., "Ultrastable CO2 Lasers", Lincoln Laboratory Journal, 3, No. 3, 479 (1990).

[11] Yangwu, M. and Liang, D., "Tunable and frequency-stablilized CO2 waveguide," Optical Engineering., 41, 12 (2002).

[12] Tuzson, B., Mohn, J., Zeeman, M.J.,Werner, R.A., Eugster, W., Zahniser, D.D. Nelson, D.D., McManus, J.B., and Emmenegger, L. "High precision and continuous field measurements of $\delta^{13}C$ and $\delta^{18}O$ in carbon dioxide with a cryogen-free QCLAS**,"** Applied Physics B, 92, 451 (2008).

[13] Weidman, D., Wysocki, G., Oppenheimer, C., and Tittel, F.K., "Development of a compact quantum cascade laser spectrometer for field measurements of CO2 isotopes," Applied Physics B, 80, 255 (2005).

[14] Nelson, D.D., Mcmanus, J.B., Hendon, S.C., Zahniser, M.S., Tuzson, B., and Emmenegger, L, "New method for isotopic ratio measurements of atmospheric carbon dioxide using a 4.3 μm pulsed quantum cascade laser," Applied Physics B, 90, 301 (2008).

[15] Regional Greenhouse Gas Initiative, an initiative of the Northeast and Mid-Atlantic States of the U.S. www.rggi.org.

[16] California Environmental Protection Agency, AIR RESOURCES BOARD, Assembly Bill 32, Global Warming Solutions Act http://www.arb.ca.gov/cc/factsheets/ab32factsheet.pdf.

[17] Marino, B. D.V., "System of Systems for monitoring greenhouse gas fluxes," US Patent Application, 2010/0198736 (2010).

[18] Marino, B. D.V., "System of Systems for monitoring greenhouse gas fluxes," US Patent Application, 2010/0198736 (2010).

[19] Lewicki, J.L., Hilley, G. E., Dobeck, L., and Marino, B.D.V., "Eddy covariance imaging of diffuse volcanic CO2 emissions at Mammoth Mountain, CA, USA," Bulletin of Volcanology, 0, published online (2011).

[20] Cook et al., "Radiocarbon studies of plant leaves and tree rings from Mammoth Mountain, CA: a long term record of magmatic CO2 release," Chemical Geology 177, 117-13 (2001).

[21] Hua, Q., & Barbetti, M., "Review of Tropospheric Bomb ^{14}C data for carbon cycle modeling and age calibration purposes," Radiocarbon Vol. 46, No. 3, 1273 (2004).

[22] Cook et al., "Radiocarbon studies of plant leaves and tree rings from Mammoth Mountain, CA: a long term record of magmatic CO2 release," Chemical Geology 177,117-131 (2001).

[23] Světlík, Ivo, Molnár, M., Váňa, M., Michálek, V. and Stefanov, P., "Estimation of $^{14}CO2$ amount in the atmosphere," Journal of Radioanalytical and Nuclear Chemistry, No. 1, 281 (2009).